

RESEARCH

Open Access



# Potential anti-tumor activity of 13.56 MHz alternating magnetic hyperthermia and chemotherapy on the induction of apoptosis in human colon cancer cell lines HT29 and HCT116 by up-regulation of Bax, cleaved caspase 3&9, and cleaved PARP proteins

Saba Jahangiri<sup>1,3</sup>, Samideh Khoei<sup>2,3\*</sup> , Sepideh Khoei<sup>4</sup>, Majid Safa<sup>5</sup>, Sakine Shirvalilou<sup>2\*</sup> and Vahid Pirhajati Mahabadi<sup>6</sup>

\*Correspondence: khoei.s@iums.ac.ir; skhoei@gmail.com; sakine.shirvaliloo@gmail.com; shirvaliloo.s@tak.iuums.ac.ir  
<sup>2</sup> Finetech in Medicine Research Center, Iran University of Medical Sciences, P.O. Box: 1449614525, Tehran, Iran  
Full list of author information is available at the end of the article

## Abstract

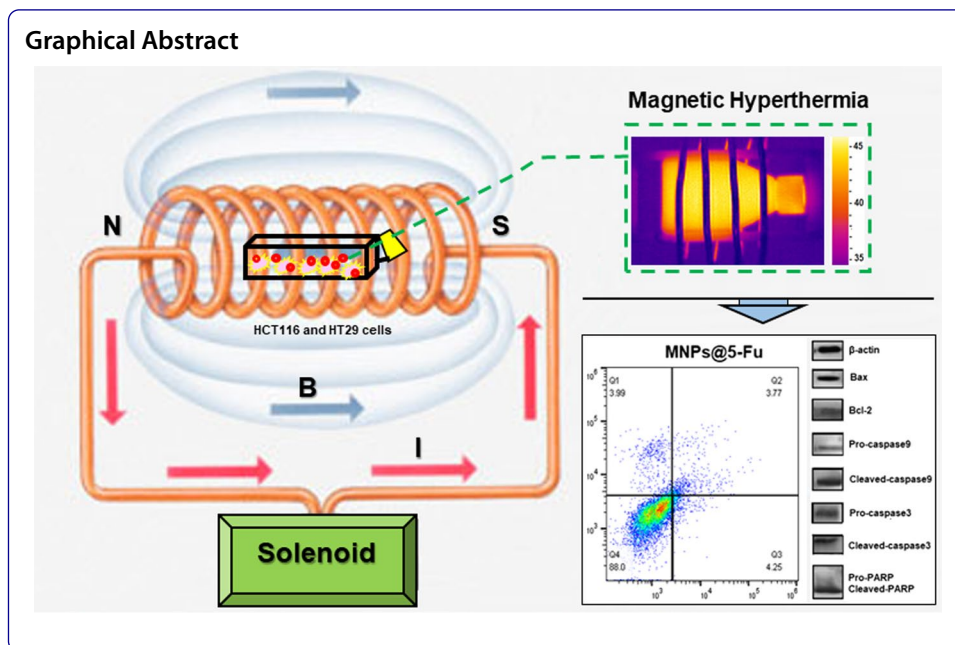
**Background:** The purpose of the present study was to evaluate the efficacy of chemo-magnetic hyperthermia (MH), a combination of alternating magnetic field (AMF) and superparamagnetic nanoparticles (SPIONs) coated with Polyethylene glycol-Poly(butyl acrylate)-Polyethylene glycol (PEG-PBA-PEG) carrying 5-Fluorouracil (5-Fu), at inducing apoptosis in the human cancer cell lines HT29 and HCT116. This process can be mediated by alterations in the expression of apoptotic effector proteins, including Bax, Bcl-2, cleaved caspase 3&9, and cleaved PARP, which are involved in the intrinsic pathway of apoptosis. For this purpose, the cells were cultured as monolayers. Then both cell lines were treated with 5-Fu/magnetic nanoparticles and magnetic hyperthermia. Finally, the effect of treatment on cancer cells was determined by Western blot analysis and flow cytometry.

**Results:** Our results showed that combined chemo-magnetic thermotherapy significantly increased the apoptosis in colon cancer cells compared to chemotherapy or hyperthermia alone ( $P < 0.05$ ). Up-regulation of Bax, cleaved caspase 3&9, and cleaved PARP proteins was indicative of apoptosis induction in cancer cells, which are involved in the intrinsic pathway of apoptosis.

**Conclusions:** This study demonstrates that localized hyperthermia was able to significantly trigger the 5-Fu release and inhibit cell viability, which, due to the synchronization of hyperthermia and chemotherapy, exacerbated the damage of cancer cells.

**Keywords:** Colon cancer, 5-fluorouracil, Magnetic hyperthermia, Apoptosis, Cleaved caspase, Cleaved PARP, Pro-PARP proteins





### Background

Alternating magnetic hyperthermia (AMH) is one of the most effective adjuvant therapeutic modalities generated by radiofrequency waves and used in combination with other modalities, such as radiotherapy and chemotherapy (Hildebrandt et al. 2002). The most challenging limitation of conventional cancer treatments, e.g., radiotherapy and chemotherapy, is that they instigate severe adverse effects in patients (Pan et al. 2020; Shirvalilou et al. 2021). Hence, today, the combined therapeutic modality (radio or chemo-thermo therapy) is increasingly being accepted as a potential treatment method in certain primary and secondary colon cancers (Grimmig et al. 2017). Research has also shown that in combination chemo-thermo therapy, the likelihood of successful treatment increases by approximately 20 to 30 percent, due to enhanced blood flow, improved oxygen and drug delivery, and pronounced tumor sensitivity (Wust et al. 2002).

In clinical treatment of colon cancer, development of resistance to chemotherapeutic agents creates a potential barrier to successful treatment of patients in advanced stages of colon cancer (Agarwal et al. 2018). On the other hand, one of the unique features of AMH is that it can be used specifically for targeted treatment of deep-seated tumors, such as glioma (Afzalipour et al. 2020), breast cancer (DeNardo et al. 2007), and colon cancer (Asadi et al. 2018). Thus, we speculated that combination of chemotherapy and AMH might significantly increase tumor cell death in the chemoresistance colon cancer cells through induction of apoptosis. Lin et al. and Jiang et al. showed that ezrin–radixin–moesin (ERM) family of proteins is overexpressed in colon cancer tumors. Radixin promotes invasion and migration of colon cancer cells by activating Rac1-ERK pathway and increasing MMP-7 production (Jiang et al. 2014; Lin et al. 2013). Protein kinase B (Akt) is activated by 5-FU and plays an important role in 5-FU chemoresistance of colon cancer cells, such as HT29 and HCT116 cells (Liu et al. 2017). Accordingly, we

studied two 5-Fu chemoresistance colon cancer cell lines, HT29 and HCT116 (He et al. 2017; Huang et al. 2019), the former of which is necrosis factor-related apoptosis-inducing ligand (TRAIL) resistant, while the latter is TRAIL sensitive (Lee et al. 2011).

To evaluate this hypothesis, we first synthesized SPION@PEG-PBA-PEG nanoparticles (MNPs) that were then loaded with 5-Fu.

5-Fu is a thymine analog with a fluorine substituent instead of methyl group, which is widely used for the treatment of malignancies (Ansfield et al. 1962; Sharp and Benefiel 1962). It is able to induce apoptosis in normal and tumoral intestinal cells (Varghese et al. 2019). However, it comes with several disadvantages, including short biological half-life, resulting from rapid metabolism of the drug, and hydrophilic nature, which renders it unable to readily pass through the cell membrane (Ortiz et al. 2012). In recent years, nanoparticles have widely been used for drug delivery, hence, the application of magnetic nanoparticles in the present study. Superparamagnetic nanoparticles (SPIONs) are one of the most important nanomaterials for induction of AMH. They can locally convert the energy of the alternating magnetic field to heat at the tumor site, thus, killing tumor cells (Kumar and Mohammad 2011; Sheervalilou et al. 2021). Intracellular magnetic hyperthermia was first proposed by Gordon et al. in 1979 (Gordon et al. 1979). The technique had more benefits than traditional hyperthermia, particularly the capability to heat malignant cells from “inside-out.” The latter could trigger cell death (apoptosis/necrosis), while simultaneously altering the function of specific proteins, rendering tumor cells more sensitive to chemotherapy or radiotherapy (Piazza et al. 2020; Rajaei et al. 2018). The current study investigates the effects of the seemingly excellent combinatorial treatment modality, consisting of chemotherapy and AMH on colon cancer cells, following the internalization of SPIONs carrying the chemotherapeutic agent (Wang et al. 2020).

In this study, the properties of the synthesized nanoparticles were analyzed to determine the size range and shape of the nanoparticles. In vitro efficacy of drug delivery, cytotoxicity, and cellular uptake of MNPs were investigated on the HT29 and HCT116 cell lines. Since previous research had demonstrated that apoptosis might be aggravated by irradiation, heat, or anti-cancer drugs (Fu et al. 2014; Mhaidat et al. 2014), in this study the Bax and Bcl-2 proteins expression were investigated by Western blotting method. Bcl-2 protein is an important inhibitor of apoptosis in cells, whereas Bax is a pro-apoptotic protein that promotes apoptosis. Therefore, an increase in Bax/Bcl-2 expression ratio indicates facilitated induction of apoptotic death (Sadeghi et al. 2019; Shirvalilou et al. 2020).

## Results

### Colon cancer cell lines

The human colon cancer cell lines HT29 and HCT116 were cultured as a monolayer in tissue culture flasks. The population doubling times were approximately  $14.72 \pm 0.41$  h and  $27.34 \pm 4.45$  h, respectively.

### Characterization of the SPION@PEG-PBA-PEG loaded with 5-Fu (MNPs@5-Fu)

The schematic profile of the final structure of the triblock copolymers (PEG-PBA-PEG) is shown in Fig. 1A. The synthesis of triblock copolymer was verified by  $^1\text{H}$  NMR spectra

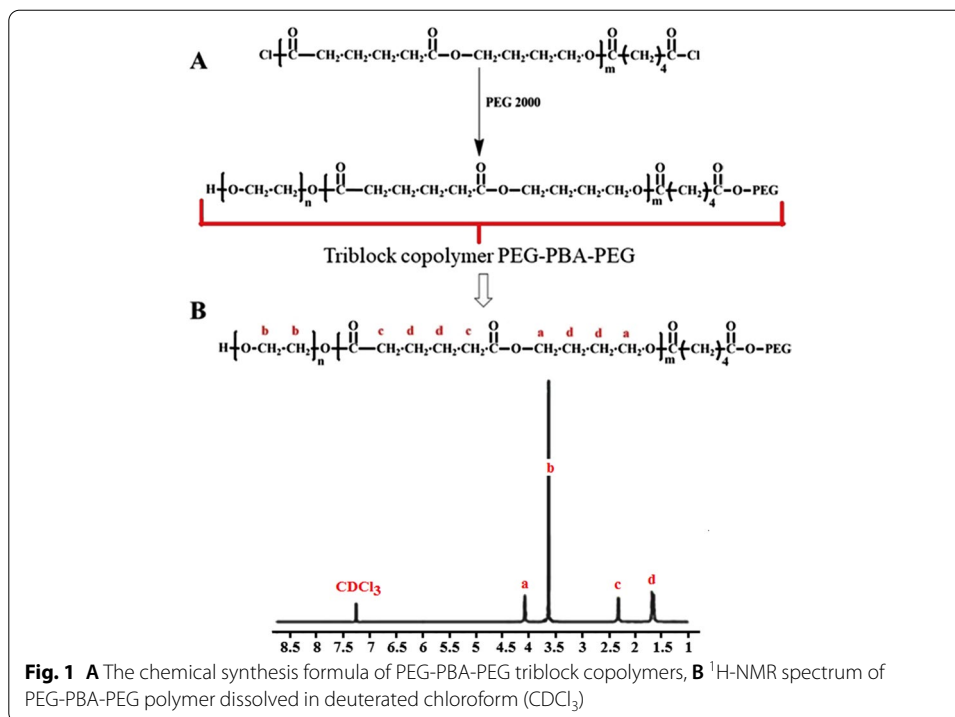


**Fig. 1** **A** The chemical synthesis formula of PEG-PBA-PEG triblock copolymers, **B** <sup>1</sup>H-NMR spectrum of PEG-PBA-PEG polymer dissolved in deuterated chloroform (CDCl<sub>3</sub>)

and observation of peaks in chemical shifts of 1.6, 2.3, 3.6, and 4.1 ppm (Fig. 1B). DLS results showed that nanoparticles with/without 5-Fu had a mean hydrodynamic size of 30–45 nm (Fig. 2A, B). The zeta potentials of MNPs and 5-Fu loaded MNPs were – 30.08 and – 28.71 mV, respectively (Table 1). The morphology of nanoparticles is shown in Fig. 2C. The TEM image of MNPs@5-Fu confirmed that the nanoparticles were spherical in size less than 30 nm. The 5-Fu loading content and encapsulation efficiency of the MNPs was 5.77% and 53.34%, respectively. Figure 2D shows the in vitro release profiles of 5-Fu from the MNPs at 37 °C and 43 °C. As can be observed, temperature had no effect on release rate. 5-Fu was released to the extent of 62.1% and 63.21% from MNPs@5-Fu nanoparticles, within approximately 72 h in a PBS at 37 °C and 43 °C, respectively.

#### In vitro cytotoxicity assay of MNPs@5-Fu nanoparticles

The cytotoxic effects of free 5-Fu and MNPs with/without drug were investigated with MTT test in the HT29 and HCT116 cell lines through the course of the 24 h treatment. The rate of cell viability as a function of 5-Fu concentration is shown in Fig. 2E, F. The results indicated that MNPs@5-Fu had a significant effect on the viability of both cell lines compared to the 5-Fu and blank MNPs (*P* < 0.05). As depicted in Fig. 2(D, E), after treatment for 24 h, the IC<sub>50</sub> values of 5-Fu, MNPs, and MNPs@5-Fu were equal to 30.58 ± 1.49, 43.55 ± 2.03, and 16.14 ± 0.22 for HT29 cells, and 13.93 ± 1.45, 20.08 ± 1.67, and 0.68 ± 1.01 μM for HCT116 cells, respectively. As shown in Fig. 2(D, E), the cytotoxicity of 5-Fu loaded MNPs in HCT116 cells was higher than that observed in the HT29 cells (*P* < 0.05).

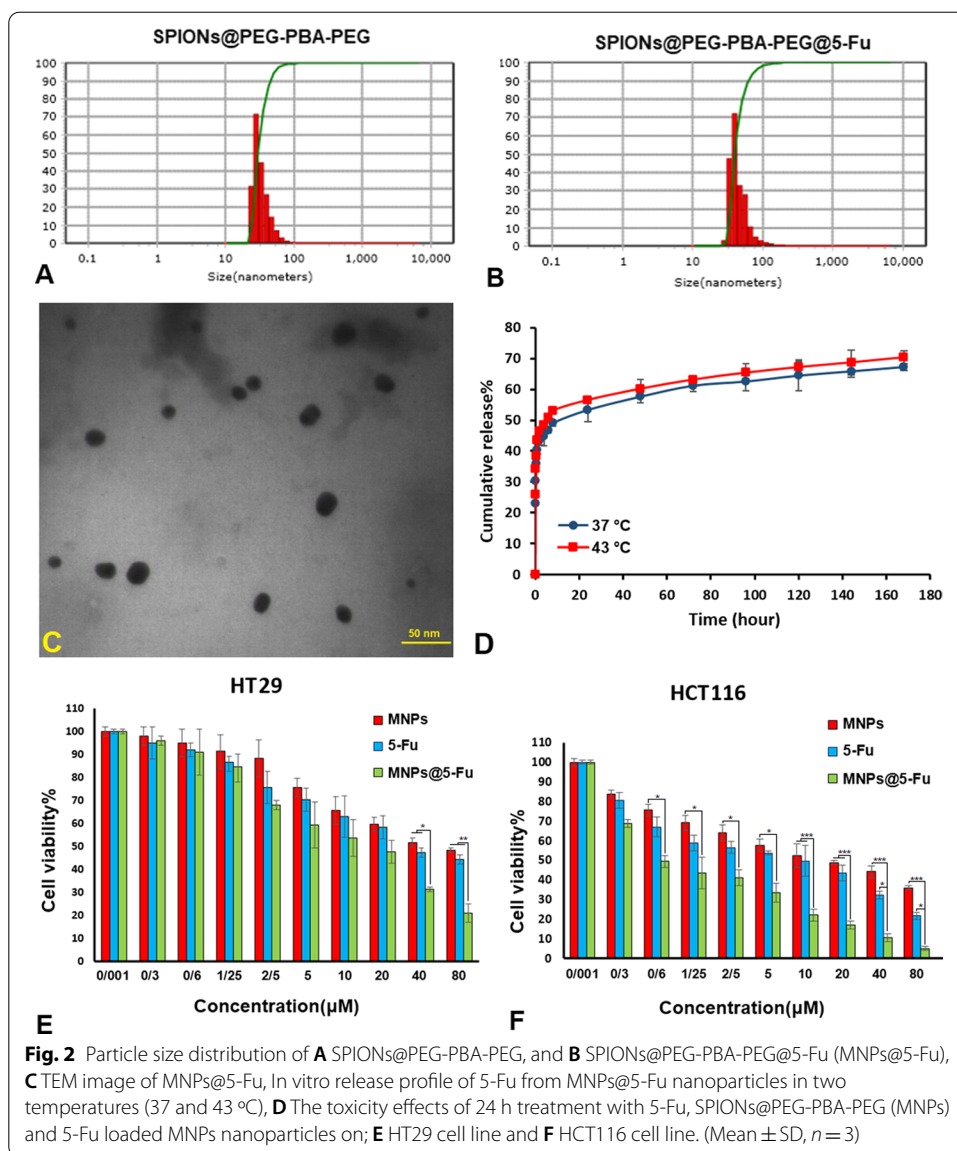


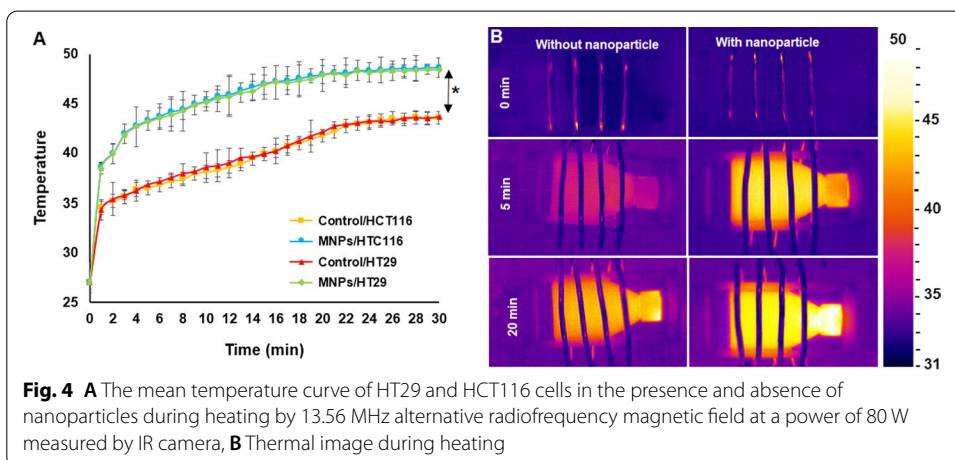
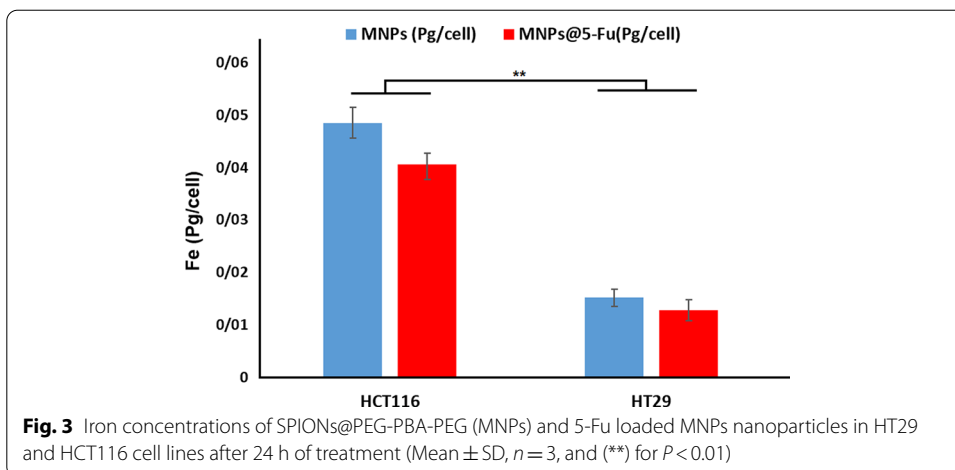
**Fig. 2** Particle size distribution of **A** SPIONs@PEG-PBA-PEG, and **B** SPIONs@PEG-PBA-PEG@5-Fu (MNPs@5-Fu), **C** TEM image of MNPs@5-Fu, In vitro release profile of 5-Fu from MNPs@5-Fu nanoparticles in two temperatures (37 and 43 °C), **D** The toxicity effects of 24 h treatment with 5-Fu, SPIONs@PEG-PBA-PEG (MNPs) and 5-Fu loaded MNPs nanoparticles on; **E** HT29 cell line and **F** HCT116 cell line. (Mean ± SD, n = 3)

**Table 1** Physico-chemical properties of nanoparticles (Mean ± SD, n = 3)

Nanoparticles	Size (nm)	Zeta Potential (mV)	Polydispersity index
SPIONs@PEG-PBA-PEG(MNPs)	32.9 ± 0.58	- 30.08 ± 1.07	0.204
SPIONs@PEG-PBA-PEG@5-Fu	44.6 ± 0.94	- 28.71 ± 1.26	0.216

**Cellular uptake of MNPs@5-Fu**

The internalization of the nanoparticles into cells was assessed through the ICP-OES analysis of HT29 and HCT116 cell lines after 24 h. The quantitative ICP-OES data are illustrated in Fig. 3. The cellular uptake of Fe was equal to 0.017 ± 0.007 and 0.042 ± 0.002 pg/cell for HT29 and HCT116 cells, respectively. Our ICP-OES results suggested that MNPs@5-Fu nanoparticles had a significantly higher affinity for entering



HCT116 cells than HT29 ( $P < 0.01$ , Fig. 3), a finding that might explain the greater toxicity of nanoparticles in HCT116 cells compared to HT29. The latter statement was confirmed by our MTT results.

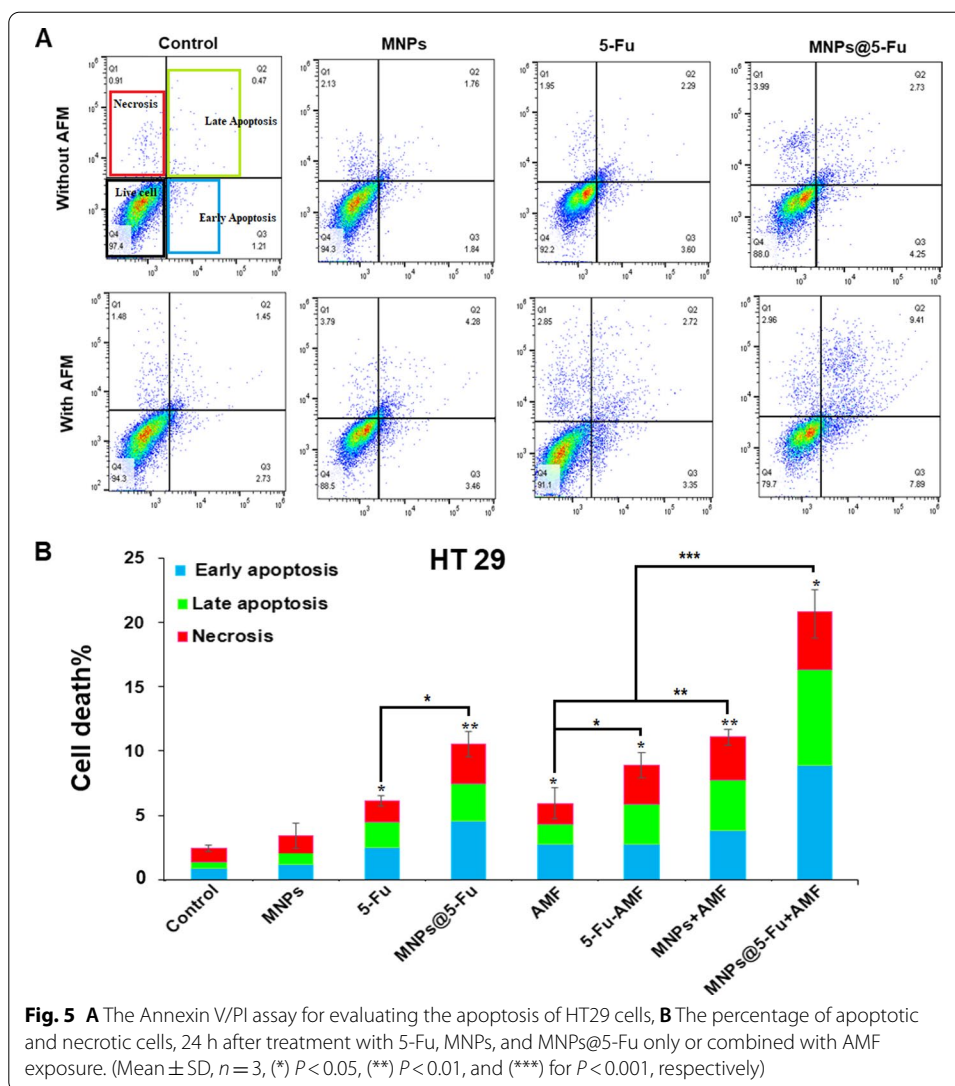
#### AMF-induced heating profile

To determine the approximate time of hyperthermia at 43 °C, the temperature changes of HT29 and HCT116 cell lines under an AMF exposure with and without MNPs@5-Fu nanoparticles were measured by IR camera. Thermometry data are visualized in Fig. 4A, B. The temperature of HT29 and HCT116 cell lines reached 43 °C after approximately 24  $\pm$  1 min of AMF exposure without the presence of nanoparticles. On the other hand, the temperature rapidly reached 43 °C within 5 min in the HT29 and HCT116 cell lines treated with MNPs@5-Fu nanoparticles.

#### In vitro anti-tumor efficacy of treatment modalities

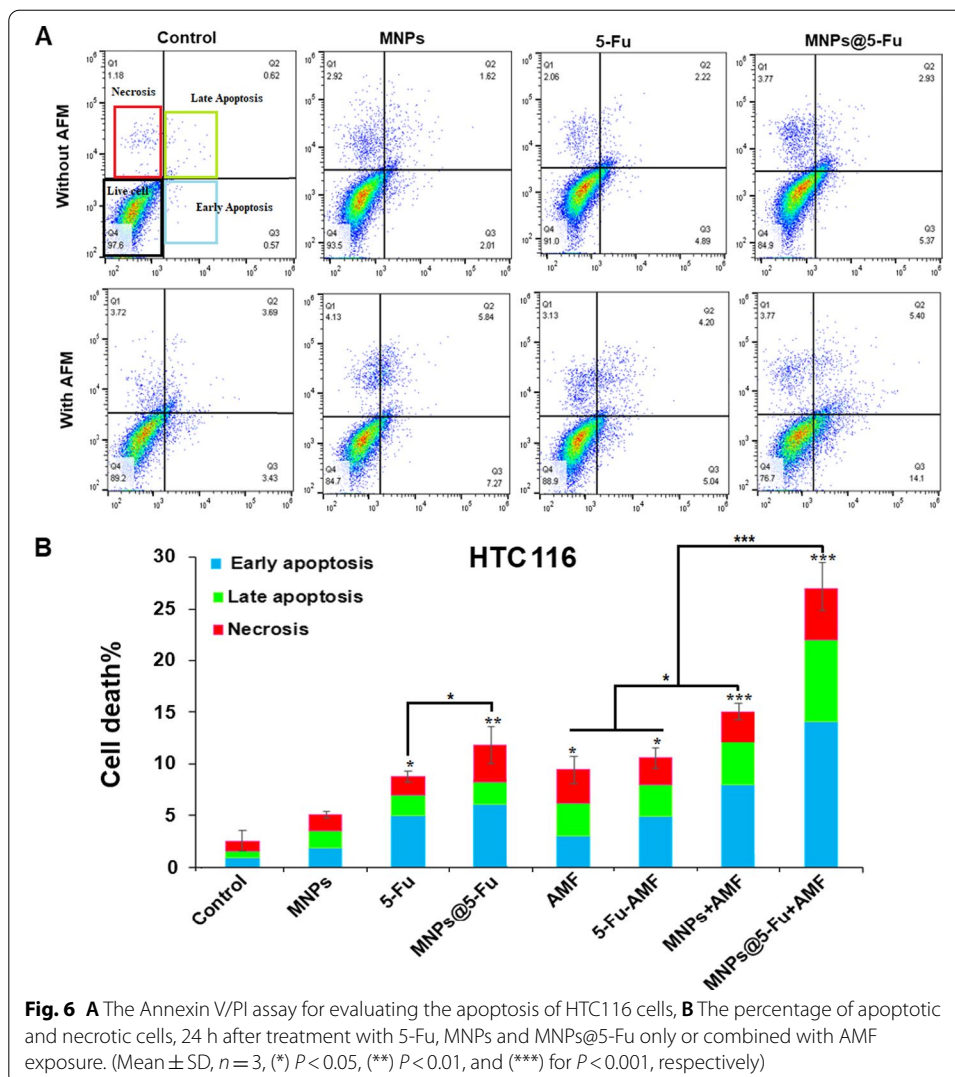
##### Flow cytometry analysis

Results of flow cytometry analysis for both cell lines are shown in Figs. 5 and 6. As flow cytometry results indicated, there was a significant difference between the control group



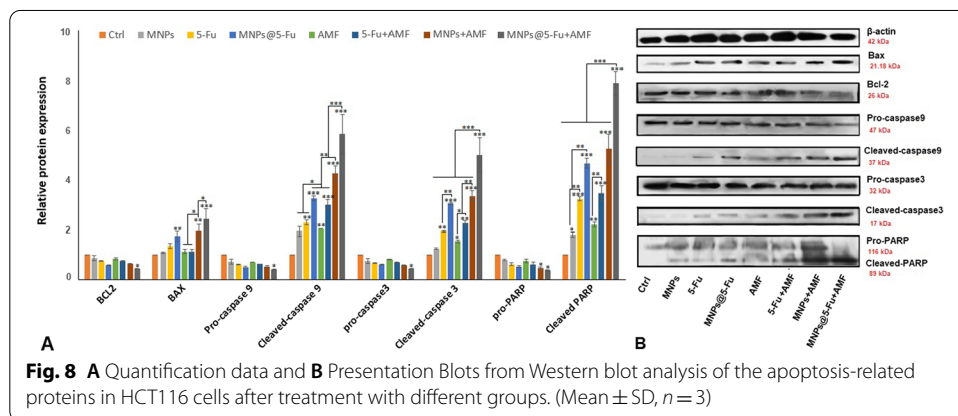
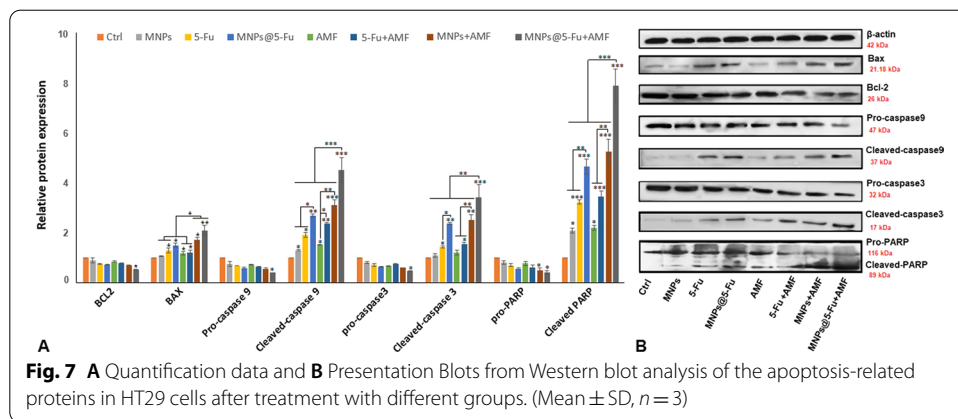
and treatment groups for both cell lines ( $P < 0.05$ ). However, there was no remarkable difference between the control group and blank MNPs for HT29 cells ( $P > 0.05$ ). The significant difference in cell death ratio was also observed between free 5-Fu and MNPs@5-Fu for HT29 and HCT116 cells ( $P < 0.03$ ), suggesting increased toxicity of the 5-Fu after being loaded onto the nanoparticles. The results clearly verified the 5-Fu-induced apoptotic death in cancer cells. On the other hand, 5-Fu or MNPs plus AMF had a significant effect on HT29 cells compared to the 5-Fu or AMF alone ( $P < 0.01$ ). Nevertheless, for HCT116 cells, only combinatorial therapy of MNPs and AMF showed a significant effect compared to single 5-Fu or MNPs alone ( $P < 0.05$ ).

Ultimately, our findings suggested that the combinatorial therapy of hyperthermia and MNPs@5-Fu could greatly increase the rate of HT29 and HCT116 cell death ( $P < 0.001$ ). As shown in Figs. 5 and 6A, B, the highest apoptosis and necrosis level (19.13% for HCT116 and 12.3% for HT29) belonged to the MNPs@5-Fu + AFM group.



### Western blot analysis

In vitro anti-tumor efficacy of different therapeutic modalities was estimated via Western blot analysis. We evaluated the expression of apoptosis-related proteins, such as Bcl-2, Bax, caspase-9, caspase-3, and PARP. As illustrated in Figs. 7 and 8A, B, an increased expression of pro-apoptotic factor, Bax, cleaved caspase-3, cleaved caspase-9, and cleaved PARP was observed in the treatment groups, compared to the control group ( $P < 0.05$ ). However, there was no significant difference between the control and MNPs group ( $P > 0.05$ ). The results also suggested the down-regulation of Bcl-2 in the treatment group of MNPs@5-Fu and AMF hyperthermia compared to control group ( $P < 0.05$ ), while there were no significant differences between the control and other groups ( $P > 0.05$ ). The highest expression of pro-apoptotic proteins and the least expression of anti-apoptotic proteins were achieved with the combinatorial treatment of MNPs@5-Fu and AMF hyperthermia ( $P < 0.001$ ). In all groups, the rate of apoptosis and necrosis of HCT116 cells was higher than HT29 cells, indicating resistance of HT29 cells to HCT116 cells, which favored the results of cell apoptosis



assay and MTT assay. The results of molecular research were in complete agreement with the flow cytometry analysis.

### Discussion

Due to the increasing prevalence of colon cancer, the present study investigated the efficiency of a combination therapy comprising 5-fluorouracil-loaded SPIONs coated with triblock copolymer PEG-PBA-PEG nanoparticles (MNPs@5-Fu), and hyperthermia. According to most studies the routine treatment for colon cancer often includes 5-Fu and additional antiplatelet drugs (Pardini et al. 2011). However, given the limitations on administration of drugs, such as systemic toxicity and the low half-life of the drug, concomitant use of chemotherapy with other therapies is thought to be as effective (Mohammadi et al. 2012). To overcome these problems in this study, we attempted to load iron nanoparticles with drugs, and take advantage of their heating properties under the magnetic field to generate local heat in cancer cells.

The size and shape of nanoparticles are important parameters in successful delivery of the drug into the cells. Based on previous studies, a size of about 10–100 nm is considered as the optimal size for proper accumulation of nanoparticles in tumor cells (Shirvalilou et al. 2020). Some researchers have also reported that a Zeta potential value of  $-30$  mV can be considered optimum for sufficient stability in the aqueous medium

(Dilnawaz et al. 2010). MNPs@5-Fu nanoparticles had an average hydrodynamic size below 50 nm and zeta potential about -30 mV (Table 1). Loading of 5-Fu into the magnetite nanoparticles increased the size of the MNPs from 33 to 45 nm, which was similar to the findings reported by Emamgholizadeh Minaeie et al. (2019). Their results showed that loading Temozolomide onto SPION-PEG-PBA-PEG increased the nanoparticle size (Minaei et al. 2019). On the other hand, loading of the drug onto the MNPs increased the half-life of the drug and further slowed down its already slow release, which ultimately increased the shelf life of the drug in the environment (Fig. 2D). Considering the confirmation of cellular uptake of nanoparticles by ICP-OES test (Fig. 3) and MTT assay data (Fig. 2E, F) it can be suggested that nanoparticles increased the toxicity of the 5-Fu by facilitating drug delivery into the cells. In Fig. 2, the lowest toxicity belongs to the nanoparticles, indicating the biocompatibility of the nanoparticles with HCT116 and HT29 cell lines. MTT results confirmed that viability of HT29 and HCT116 cells treated with SPIONs coated triblock copolymer PEG-PBA-PEG was more than 70% at a high concentration (8  $\mu$ M and 1  $\mu$ M, respectively) for 24 h, while 5-Fu loaded MNPs were shown to have a significantly higher toxicity than the blank MNPs (Fig. 2E, F). This could indicate the negligible toxicity of synthesized SPIONs coated triblock copolymer PEG-PBA-PEG. Similar results have been reported by Kim et al. and Lee et al., highlighting the good cell biocompatibility and low toxicity of copolymer polymers mPEG-PBA (at high concentrations  $\geq 200$   $\mu$ g/mL) (Kim et al. 2016), and PEG coating on SPIO nanoparticles ( $\geq 50$   $\mu$ g/mL) (Dulińska-Litewka et al. 2019), respectively. Figure 2E, F shows that HCT-116 cells were more sensitive to 5-Fu and MNPs with/without drug compared to HT-29 cells. Mhaidat et al. indicated that HCT116 colon cancer cells had the greatest sensitivity to 5-Fu, while the HT29 cells were less sensitive to 5-Fu (Mhaidat et al. 2014). Ravizza et al. (2004) demonstrated that the HT29 cells carrying a mutant form of the p53 gene were more resistant to the DOX toxicity than the HCT116 cells. Golbaz et al. suggested that HCT116 cells were very sensitive to X-rays, while HT29 cells were more resistant to X-rays (Golbaz et al. 2020).

Following the synthesis and characterization of the nanoparticles, therapeutic approaches were tested on the two colon cancer cell lines (HT29 and HCT116) to evaluate the therapeutic efficacy of chemo-hyperthermia. Since both 5-Fu and hyperthermia treatments induce apoptosis in the cells (Mustafa et al. 2013), the rate of apoptotic death in the two cell lines was evaluated by flow cytometry and Western blot assay.

Caspases are a group of proteins presented by the cysteine protease family that modulate the apoptotic response (Kumar 1999). Caspase-3 is a major mediator of apoptosis, which is activated by an initiator caspase-9. Activated caspases break down many cellular substrates, such as PARP, eventually leading to cell death (Slee et al. 2001). The results of flow cytometry showed that the simultaneous application of AMF and 5-Fu increased the number of cells undergoing apoptosis compared to 5-Fu or AMF alone ( $P < 0.05$ , Figs. 5 and 6). The results indicated that magnetic hyperthermia improved the efficacy of chemotherapy, which could be due to the constructive effect of hyperthermia on the permeability of the cell membrane to the chemotherapeutic agents (Mériida et al. 2020). The combinational treatment of MNPs and AMF hyperthermia resulted in more cytotoxicity than MNPs, and AMF alone ( $P < 0.05$ , Figs. 5, 6, 7 and 8). Accordingly, Mustafa et al. (2013) reported that when the human breast adenocarcinoma cancer cells were

exposed to RF hyperthermia (high frequency of 13.56 MHz or low frequency of 350 kHz) in the presence of iron nanoparticles for 20 min, cell death was significantly increased compared to RF treatment alone (Mustafa et al. 2013). In fact, the results of this study, compared to the study by Golbaz et al. (2020), confirmed that magnetic nanoparticles in combination with hyperthermia are much more efficient than in combination with X-rays. On the other hand, the combinatorial therapy of 5-Fu and AMF hyperthermia showed a greater effect on HT29 cells ( $P < 0.05$ ) than on HCT116 cells ( $P > 0.05$ ) compared to single therapies of 5-Fu or AMF. This may be due to the high resistance of HT29 cells to 5-Fu treatment (He et al. 2017; Lee et al. 2011). Consistently, Zamora-Mora et al. showed that the 5-Fu, along with the AMF, had a significant effect on A172 cells, while no such effect was reported for FBH cells compared to the drug alone (Zamora-Mora et al. 2017). Ultimately, our in vitro results showed that colon cancer cells (HCT116 and HT29) could be significantly destroyed when exposed to MNPs@5-Fu nanoparticles and AMF hyperthermia. The highest induction of apoptosis (14.06% for HCT116 and 8.87% for HT29) was obtained in this treatment group. Investigation of the mechanism of action showed that this treatment method could induce apoptosis in human colon adenocarcinoma HCT116 and HT29 cell lines by up-regulating the level of Bax, cleaved caspase-9, cleaved caspase-3, and cleaved PARP, while down-regulating the levels of Bcl-2, Pro-caspase 9, and Pro-PARP. Wang et al. (2007) and Liang et al. (2007) had already shown that the up-regulation of Bax and down-regulation of Bcl-2 could be enhanced by the activation of mitochondrial apoptotic pathway under hyperthermia combined with chemotherapy.

## Conclusions

This study presents the assessment of size, surface charge, toxicity, and pharmacokinetics of synthesized magnetic nanocarriers. The results showed that MNPs have low toxicity in both HT29 and HCT116 cell lines. Also, our study showed that chemotherapy with magnetic nanoparticles coated with triblock copolymers PEG-PBA-PEG, as a 5-fluorouracil carrier, combined with alternating magnetic field hyperthermia significantly induced the apoptosis in the chemoresistant HT29 and HCT116 cell lines through up-regulation of Bax, activation of caspase-3, caspase-9, PARP, and down-regulation of Bcl-2.

## Methods

### Cell line and monolayer culture

The human colonic adenocarcinoma cell lines HT29 and HCT116 were purchased from Pasteur Institute of Iran. Cells were cultured in RPMI-1640 complete medium (Thermo Fisher Scientific, GIBCO, USA) with 10% fetal bovine serum (FBS) (Bovogen Biologicals Pty Ltd, Australia), penicillin (100 units/mL), and streptomycin (100 µg/mL, GIBCO). The HT29 and HCT116 cells ( $10^4$  cells/cm<sup>2</sup>) were cultured in the T-25 tissue culture flasks (Orange Scientific, Braine l'Alleud, Belgium). The cultures were maintained in incubator (Memmert GmbH+Co. KG, Germany) with a 5% CO<sub>2</sub> and temperature of 37 °C.

## Synthesis and characterization of nanoparticles

### Synthesis of copolymer PEG (2000)-Poly(butylene adipate)-PEG (2000), (PEG-PBA-PEG)

PEG (2000)-Poly(butylene adipate)-PEG (2000) was produced by polycondensation reaction of 1,4-butylene glycol and adipoyl chloride under solvent-free conditions. The reaction was initiated by adding 0.9 mL (0.65 g, 6.5 mmol) of triethylamine to 1.58 mL (1.98 g, 10.815 mmol) of adipoyl chloride and 0.91 mL (0.93 g, 10.3 mmol) of 1,4-butanediol at 85 °C on the magnetic stirrer overnight (until no more HCl was released) (Khoee et al. 2007). When the acid chloride to alcohol ratio increased (1.05:1), the end groups of the polymers would be the acid chloride groups. Then, excess amount of PEG was mixed with the polyester. The product was precipitated in 40 mL diethyl ether at 15 °C, rinsed 3 times with distilled water (3 × 30 mL), and then separated by centrifugation. The synthesis of PEG-PBA-PEG polymer was dried at a reduced temperature for 10 h and then confirmed by <sup>1</sup>H NMR spectra (Fig. 1).

### Preparation of Fe<sub>3</sub>O<sub>4</sub>@PEG-PBA-PEG@5-Fu nanoparticles by double emulsion method

Dual emulsion (w/o/w) method was used to produce the Fe<sub>3</sub>O<sub>4</sub>@PEG-PBA-PEG@5-Fu nanoparticles. At first, 30 mg of Fe<sub>3</sub>O<sub>4</sub> nanoparticles was suspended in 7 mL of dichloromethane, and then PEG-PBA-PEG polymer (50 mg) and Span 60 (200 mg) were added to the mixture. After, 10 mg of 5-Fu was dissolved in the mixture of deionized water and Tween 60, and this solution was added to polymer coated Fe<sub>3</sub>O<sub>4</sub> nanoparticles (MNPs) suspension and sonicated for 30 s. The emulsion was added to a solution containing deionized water (15 mL) and glycerol (15 mL) and, mechanically stirred for 3 h. The obtained nanoparticles were then separated using a magnet, and then washed twice with deionized water. The product was dried for 12 h using a freeze dryer.

The blank nanoparticles were synthesized in exactly the same method, only without the addition of 5-Fu.

### Characterization of the nanoparticles

Hydrodynamic size and zeta potential of the nanoparticles (Fe<sub>3</sub>O<sub>4</sub>@PEG-PBA-PEG, Fe<sub>3</sub>O<sub>4</sub>@PEG-PBA-PEG@5-Fu) were evaluated by Zeta sizer analyzer (Nanoflex, nano-Care Company, Germany). The morphology of the nanoparticles was determined by a Transmission Electron Microscope (TEM) (Zeiss LEO906, Carl Zeiss company, Germany). In addition, the nanoparticle size distribution was extracted from TEM images by Image J software.

Next, to determine the drug loading capacity (DLC) and encapsulation efficiency (EE), 3.9 mg of MNP@5-Fu nanoparticles was suspended in acetone and the 5-Fu concentration was determined by a UV spectrophotometer (Pharmacia Biotech, SPW Industrial, USA) at a 256 nm wavelength. The DLC and EE properties were determined according to Eqs. 1 and 2, respectively:

$$\text{DLC (\%)} = \left( \frac{\text{Amount of 5-Fu in the nanoparticles}}{\text{Nanoparticles weight}} \right) \times 100, \quad (1)$$

$$\text{EE (\%)} = \left( \frac{\text{Amount of 5-Fu in the nanoparticles}}{\text{Total amount of 5-Fu in the feeding}} \right) \times 100. \quad (2)$$

Finally, to determine the 5-Fu release profile from nanoparticles (MNPs@5-Fu) in PBS (release medium, pH ~ 7.4), dialysis bag (MWCO 12, 400 Da) diffusion method was used. Concentration of 5-Fu loaded on the nanoparticles was determined using a UV spectrophotometer at 256 nm.

#### **In vitro cytotoxicity assay**

The cytotoxicity of the two types of nanoparticles (MNPs, MNPs@5-Fu) and free 5-Fu in the HT29 and HCT116 cells was investigated using MTT assay. The cell lines were cultured in a 96-well plate (5000 cells/well) overnight. Then, the cells were treated with 5-Fu (0.01–100  $\mu$ M) and the nanoparticles with/without drug at equivalent 5-Fu concentrations (0.65 to 20.81  $\mu$ g/mL) for 24 h. Three wells with untreated cells were used as control group. Next, the wells were rinsed twice with cold PBS solution, and MTT solution (100  $\mu$ L) was added to each well, which was then incubated for 4 h. The MTT dye was then removed, and 100  $\mu$ L of DMSO solution was added to each well and shaken for 20 min. The absorbance was measured with an ELISA Reader set to 570 nm. Cell viability charts were plotted against different drug concentrations and inhibitory concentration (IC<sub>50</sub>) was calculated.

#### **Cellular uptake of nanoparticles**

Inductively coupled plasma optical emission spectroscopy (ICP-OES) was used to measure the amount of nanoparticles uptake into the HT29 and HCT116 cells. Cells ( $2 \times 10^6$  cell/flask) were seeded in T-25 flasks for 24 h and then treated with a concentration of 0.859  $\mu$ g/mL of nanoparticles with/without 5-Fu. After treatment for 24 h, the cells were rinsed with cold PBS to be eliminated of suspended nanoparticles. Cells were trypsinized, counted, and then digested with HNO<sub>3</sub> (500  $\mu$ L) at 150 °C for 2 h. Finally, the iron concentration in the samples was determined by an ICP-OES test (Vista Pro, Varian, Australia).

#### **Heating profile of Magnetic hyperthermia**

In order to determine the time required for magnetic hyperthermia (at 43 °C) by application of AMF, the temperature changes of both cells were evaluated using an infrared (IR) thermal camera. The HT29 and HCT116 cell lines were cultured in T-25 flasks. After 24 h, 0.3  $\mu$ g/mL of free 5-Fu or 0.859  $\mu$ g/mL of MNPs was added to the culture medium. After 24 h, the treated cells were rinsed with cold PBS and fresh RPMI medium was replaced. The samples (treated and controlled) were then placed in a circular RF coil and exposed with an alternating magnetic field (13.56 MHz, 40 A/m). The temperature changes of the cells were monitored using an IR camera (875-2i, Testo, UK) and the temperature–time curve was plotted.

#### **Therapeutic efficiency of different treatment modalities**

The cytotoxic effects of chemotherapy, nanoparticles, and AMF hyperthermia alone or in combination were investigated on the HT29 and HCT116 cell lines. In our study,

eight treatment groups were evaluated: (1) control; (2) free 5-Fu (0.3  $\mu\text{g}/\text{mL}$  ~IC10); (3) MNPs (0.859  $\mu\text{g}/\text{mL}$ ); (4) MNPs@5-Fu (0.859  $\mu\text{g}/\text{mL}$  containing 0.3  $\mu\text{g}/\text{mL}$  of 5-Fu); (5) AMF hyperthermia (13.56 MHz, 80 W); (6) MNPs + AMF; (7) 5-Fu + AMF; and (8) MNPs@5-Fu.

The HT29 and HCT116 cell lines were seeded into T-25 flasks. After 24 h, the cells were treated with different treatment modalities. According to the time–temperature curve, the AMF exposure time in combination with nanoparticles was 5 min for both cell lines. However, when AMF was applied alone, the exposure time was 23 min for HT29 and 24 min for HCT116. Finally, the toxicity effects of different treatments modalities were evaluated using the Annexin V-FITC/PI fluorescent kit, and Western blotting analysis. All treatments were repeated three times.

### **In vitro anti-tumor efficacy of nanoparticles**

#### **Cell apoptosis assay**

To determine the cell apoptosis induced by different therapeutic methods on the HT29 and HCT116 cell lines, cells were cultured and treated. After 24 h of treatment, cells were detached, rinsed with cold PBS, and suspended in the ice-cold 1X binding buffer. After that, FITC Annexin V (5  $\mu\text{L}$ ) was added to each sample, and the samples were incubated at 25 °C in the dark for 15 min. Then, propidium iodide (5  $\mu\text{L}$ ) was added to each sample, and the cells were evaluated with BD FACS Caliber flow cytometry device (BD, San Jose, USA). Finally, the percentage of apoptotic and necrotic cells in each sample was analyzed and calculated.

#### **Western blotting**

Western blotting method was performed for analyzing the protein expression. In summary, the cells were lysed on ice by a RIPA Buffer mixed with PhosStop (Roche Applied Science, Germany), protease inhibitors (Roche Applied Science, Germany), and PMSF (Merck KGaA, Germany). Concentration of the total protein extracted from the treated cells was measured with Pierce BCA Protein Assay Kit (Thermo Fisher Scientific, USA). ALL samples were uniformly loaded with equal amounts of sample protein. Proteins were separated by SDS–polyacrylamide gel electrophoresis (SDS-PAGE) and blotted onto a PVDF membrane (Millipore, Merck, Germany). Membranes were probed with specific primary antibodies and Rabbit polyclonal Secondary Antibody to Sheep IgG—H&L (HRP) (ab97130, 1:5000 dilution, Abcam, Cambridge, MA, USA). Then, chemiluminescent signals were visualized for bands with horseradish peroxidase (HRP) substrate (Merck KGaA, Germany). The following antibodies were used: Bcl-2 (ab196495, 1:1000 dilution); Bax (ab32503, 1:5000); cleaved caspase-9 (ab202068, 1:2000); cleaved caspase-3 (ab32351, 1:5000, Abcam); and cleaved PARP (ab191217, 1:1000). These antibodies were purchased from Abcam Company (Abcam, Cambridge, MA, USA).  $\beta$ -actin (#4967, 1:1000,) was purchased from Cell Signaling Technology (CST) company (Beverly, MA, USA) (all the resulting protein bands were visualized using ECL Western Blotting Detection Reagent (ChemiDocXRS; Bio-Rad, USA) and quantified by densitometry using ImageJ software and normalized to that of  $\beta$ -actin protein. In quantitative Western blotting analysis, target proteins (Bax, Bcl-2, caspase 3&9, and PARP) were measured in samples treated by various treatment modalities. The

intensity of each target protein band is then divided by the intensity of the housekeeping protein ( $\beta$ -actin). The ratio of the target protein to  $\beta$ -actin was then used to compare target protein abundance in samples of different treatment groups (Degaspero et al. 2014).

### Statistical analysis

All results were measured as the mean  $\pm$  standard deviation (SD). Statistical significance for the thermometry analysis (Fig. 4) was measured with unpaired Student's t-test, and for the ICP test (Fig. 3), cell death assays (Figs. 2, 5 and 6) and Western blotting results (7&8) were determined using one-way ANOVA method followed by a Tukey post hoc test when comparing all pairs of groups, using SPSS version 22. \* $P < 0.05$  was considered to be statistically significant.

### Abbreviations

MH: Magnetic hyperthermia; AMF: Alternating magnetic field; 5-Fu: 5-Fluorouracil; SPIONs: Superparamagnetic nanoparticles; MNPs: PEG-PBA-PEG superparamagnetic nanoparticles.

### Acknowledgements

Not applicable.

### Authors' contributions

All the authors contributed to the study conception and design. SK, MS, and VPM contributed to material preparation. SJ, SS, and SK conducted the experiments and collected the data. The first draft of the manuscript was written by SJ and SS. All the authors reviewed the manuscript. All aspects of this study were supervised by SK. All authors read and approved the final manuscript.

### Funding

This work was supported by a Grant No.32493 from Iran University of Medical Sciences (IUMS).

### Availability of data and materials

The datasets used and/or analyzed during the current study are available from the corresponding author on reasonable request.

### Declarations

#### Ethics approval and consent to participate

This research was approved by Ethics Committee of Iran University of Medical Sciences. Human cell lines used in this study do not require ethics approval.

#### Consent for publication

Not applicable.

#### Competing interests

The authors declare that they have no competing interests.

#### Author details

<sup>1</sup>Student Research Committee, Iran University of Medical Sciences, Tehran, Iran. <sup>2</sup>Finetech in Medicine Research Center, Iran University of Medical Sciences, P.O. Box: 1449614525, Tehran, Iran. <sup>3</sup>Department of Medical Physics, School of Medicine, Iran University of Medical Sciences, Tehran, Iran. <sup>4</sup>Department of Polymer Chemistry, School of Chemistry, College of Science, University of Tehran, Tehran, Iran. <sup>5</sup>Department of Hematology and Blood Transfusion, Faculty of Allied Medicine, Iran University of Medical Sciences, Tehran, Iran. <sup>6</sup>Neuroscience Research Center, Iran University of Medical Sciences, Tehran, Iran.

Received: 1 September 2021 Accepted: 28 November 2021

Published online: 17 December 2021

### References

- Afzalipour R, Khoei S, Khoee S, Shirvalilou S, Raoufi NJ, Motevalian M, Karimi MY (2020) Thermosensitive magnetic nanoparticles exposed to alternating magnetic field and heat-mediated chemotherapy for an effective dual therapy in rat glioma model. *Nanomed Nanotechnol Biol Med* 31:102319
- Agarwal A et al (2018) Curcumin induces apoptosis and cell cycle arrest via the activation of reactive oxygen species-independent mitochondrial apoptotic pathway in Smad4 and p53 mutated colon adenocarcinoma HT29 cells. *Nutr Res* 51:67–81
- Ansfield FJ, Schroeder JM, Curreri AR (1962) Five years clinical experience with 5-fluorouracil. *JAMA* 181:295–299

- Asadi L, Shirvallilou S, Khoee S, Khoei S (2018) Cytotoxic effect of 5-fluorouracil-loaded polymer-coated magnetite nanoparticle combined with radiofrequency. *Anti-Cancer Agents Med Chem* 18:1148–1155
- Degasperi A, Birtwistle MR, Volinsky N, Rauch J, Kolch W, Kholodenko BN (2014) Evaluating strategies to normalise biological replicates of Western blot data. *PLoS ONE* 9:e87293
- DeNardo SJ et al (2007) Thermal dosimetry predictive of efficacy of <sup>111</sup>In-ChL6 nanoparticle AMF-induced thermoablative therapy for human breast cancer in mice. *J Nuclear Med* 48:437–444
- Dilnawaz F, Singh A, Mohanty C, Sahoo SK (2010) Dual drug loaded superparamagnetic iron oxide nanoparticles for targeted cancer therapy. *Biomaterials* 31:3694–3706
- Dulińska-Litewka J, Łazarczyk A, Hałubiec P, Szafrński O, Karnas K, Karewicz A (2019) Superparamagnetic iron oxide nanoparticles—current and prospective medical applications. *Materials* 12:617
- Fu Y et al (2014) Antioxidants decrease the apoptotic effect of 5-Fu in colon cancer by regulating Src-dependent caspase-7 phosphorylation. *Cell Death Dis* 5:e983–e983
- Golbaz R, Khoei S, Khoee S, Shirvallilou S, Safa M, Mahdavi SR, Karimi MR (2020) Apoptosis pathway in the combined treatment of x-ray and 5-FU-loaded triblock copolymer-coated magnetic nanoparticles. *Nanomedicine* 15:2255–2270
- Gordon R, Hines J, Gordon D (1979) Intracellular hyperthermia a biophysical approach to cancer treatment via intracellular temperature and biophysical alterations. *Med Hypotheses* 5:83–102
- Grimmig T et al (2017) Upregulated heat shock proteins after hyperthermic chemotherapy point to induced cell survival mechanisms in affected tumor cells from peritoneal carcinomatosis. *Cancer Growth Metastasis* 10:1179064417730559
- He J, Pei L, Jiang H, Yang W, Chen J, Liang H (2017) Chemoresistance of colorectal cancer to 5-fluorouracil is associated with silencing of the BNIP3 gene through aberrant methylation. *J Cancer* 8:1187
- Hildebrandt B et al (2002) The cellular and molecular basis of hyperthermia. *Crit Rev Oncol Hematol* 43:33–56
- Huang C-Y, Huang C-Y, Pai Y-C, Lin B-R, Lee T-C, Liang P-H, Yu LC-H (2019) Glucose metabolites exert opposing roles in tumor chemoresistance. *Front Oncol* 9:1282
- Jiang Q-H, Wang A-X, Chen Y (2014) Radixin enhances colon cancer cell invasion by increasing MMP-7 production via Rac1-ERK pathway. *Sci World J*. <https://doi.org/10.1155/2014/340271>
- Khoee S, Hassanzadeh S, Goliaie B (2007) Effects of hydrophobic drug–polyesteric core interactions on drug loading and release properties of poly (ethylene glycol)–polyester–poly (ethylene glycol) triblock core–shell nanoparticles. *Nanotechnology* 18:175602
- Kim J, Lee YM, Kim H, Park D, Kim J, Kim WJ (2016) Phenylboronic acid-sugar grafted polymer architecture as a dual stimuli-responsive gene carrier for targeted anti-angiogenic tumor therapy. *Biomaterials* 75:102–111
- Kumar S (1999) Regulation of caspase activation in apoptosis: implications in pathogenesis and treatment of disease. *Clin Exp Pharmacol Physiol* 26:295–303
- Kumar CS, Mohammad F (2011) Magnetic nanomaterials for hyperthermia-based therapy and controlled drug delivery. *Adv Drug Deliv Rev* 63:789–808
- Lee SC et al (2011) Low-dose combinations of LBH589 and TRAIL can overcome TRAIL-resistance in colon cancer cell lines. *Anticancer Res* 31:3385–3394
- Liang H, Zhan H-J, Wang B-G, Pan Y, Hao X-S (2007) Change in expression of apoptosis genes after hyperthermia, chemotherapy and radiotherapy in human colon cancer transplanted into nude mice. *World J Gastroenterol* 13:4365
- Lin M-C, Tsai S-Y, Wang F-Y, Liu F-H, Syu J-N, Tang F-Y (2013) Leptin induces cell invasion and the upregulation of matrix metalloproteinase-1 in human colon cancer cells. *Biomedicine* 3:174–180
- Liu N et al (2017) MicroRNA-302a enhances 5-fluorouracil-induced cell death in human colon cancer cells. *Oncol Rep* 37:631–639
- Mérida F, Rinaldi C, Juan EJ, Torres-Lugo M (2020) In vitro ultrasonic potentiation of 2-phenylethanesulfonamide/magnetic fluid hyperthermia combination treatments for ovarian cancer. *Int J Nanomed* 15:419
- Mhaidat NM, Bouklihacene M, Thorne RF (2014) 5-Fluorouracil-induced apoptosis in colorectal cancer cells is caspase-9-dependent and mediated by activation of protein kinase C-δ. *Oncol Lett* 8:699–704
- Minaii SE, Khoei S, Khoee S (2019) Tri-block copolymer nanoparticles modified with folic acid for temozolomide delivery in glioblastoma. *Int J Biochem Cell Biol* 108:72–83
- Mohammadi S, Khoei S, Mahdavi SR (2012) The combination effect of poly (lactic-co-glycolic acid) coated iron oxide nanoparticles as 5-fluorouracil carrier and X-ray on the level of DNA damages in the DU 145 human prostate carcinoma cell line. *J Bionanosci* 6:23–27
- Mustafa T et al (2013) Iron oxide nanoparticle-based radio-frequency thermotherapy for human breast adenocarcinoma cancer cells. *Biomater Sci* 1:870–880
- Ortiz R et al (2012) 5-Fluorouracil-loaded poly (ε-caprolactone) nanoparticles combined with phage E gene therapy as a new strategy against colon cancer. *Int J Nanomed* 7:95
- Pan J et al (2020) Combined magnetic hyperthermia and immune therapy for primary and metastatic tumor treatments. *ACS Nano*. <https://doi.org/10.1021/acsnano.9b08550>
- Pardini B et al (2011) 5-Fluorouracil-based chemotherapy for colorectal cancer and MTHFR/MTRR genotypes. *Br J Clin Pharmacol* 72:162
- Piazza RD et al (2020) PEGlatyon-SPION surface functionalization with folic acid for magnetic hyperthermia applications. *Mater Res Express*. <https://doi.org/10.1088/2053-1591/ab6700>
- Rajaei Z, Khoei S, Mahdavi SR, Ebrahimi M, Shirvallilou S, Mahdavian A (2018) Evaluation of the effect of hyperthermia and electron radiation on prostate cancer stem cells. *Radiat Environ Biophys* 57:133–142
- Ravizza R, Gariboldi MB, Passarelli L, Monti E (2004) Role of the p53/p21 system in the response of human colon carcinoma cells to Doxorubicin. *BMC Cancer* 4:92
- Sadeghi S et al (2019) Anti-cancer effects of cinnamon: Insights into its apoptosis effects. *Eur J Med Chem*. <https://doi.org/10.1016/j.ejmech.2019.05.067>
- Sharp GS, Benefiel WW (1962) 5-Fluorouracil in the treatment of inoperable carcinoma of the colon and rectum. *Cancer Chemother Rep* 20:97–101

- Sheervalilou R, Shirvaliloo M, Sargazi S, Ghaznavi H (2021) Recent advances in iron oxide nanoparticles for brain cancer theranostics: from in vitro to clinical applications. *Expert Opin Drug Deliv*. <https://doi.org/10.1080/17425247.2021.1888926>
- Shirvalilou S, Khoei S, Khoee S, Mahdavi SR, Raoufi NJ, Motevalian M, Karimi MY (2020) Enhancement radiation-induced apoptosis in C6 glioma tumor-bearing rats via pH-responsive magnetic graphene oxide nanocarrier. *J Photochem Photobiol B Biol* 205:111827
- Shirvalilou S, Khoei S, Esfahani AJ, Kamali M, Shirvaliloo M, Sheervalilou R, Mirzaghavami P (2021) Magnetic Hyperthermia as an adjuvant cancer therapy in combination with radiotherapy versus radiotherapy alone for recurrent/progressive glioblastoma: a systematic review. *J Neuro-Oncol*. <https://doi.org/10.1007/s11060-021-03729-3>
- Slee EA, Adrain C, Martin SJ (2001) Executioner caspase-3, -6, and -7 perform distinct, non-redundant roles during the demolition phase of apoptosis. *J Biol Chem* 276:7320–7326
- Varghese V et al (2019) FOXM1 modulates 5-FU resistance in colorectal cancer through regulating TYMS expression. *Sci Rep* 9:1–16
- Wang J-M, Xiao B-L, Zheng J-W, Chen H-B, Zou S-Q (2007) Effect of targeted magnetic nanoparticles containing 5-FU on expression of bcl-2, bax and caspase 3 in nude mice with transplanted human liver cancer. *World J Gastroenterol* 13:3171
- Wang R et al (2020) The cell uptake properties and hyperthermia performance of ZnO, 5Fe<sub>2</sub>O<sub>4</sub>/SiO<sub>2</sub> nanoparticles as magnetic hyperthermia agents. *R Soc Open Sci* 7:191139
- Wust P et al (2002) Hyperthermia in combined treatment of cancer. *Lancet Oncol* 3:487–497
- Zamora-Mora V et al (2017) Chitosan nanoparticles for combined drug delivery and magnetic hyperthermia: From preparation to in vitro studies. *Carbohydr Polym* 157:361–370

### **Publisher's Note**

Springer Nature remains neutral with regard to jurisdictional claims in published maps and institutional affiliations.